

Crystalline Morphology and Crystallization Kinetics of Melt-miscible Crystalline/Crystalline Polymer Blends of Poly(vinylidene fluoride) and Poly(butylene succinate-co-24mol% hexamethylene succinate)^{*}

Gu-yu Wang and Zhao-bin Qiu^{**}

State Key Laboratory of Chemical Resource Engineering, Key Laboratory of Carbon Fiber and Functional Polymers,
Ministry of Education, Beijing University of Chemical Technology, Beijing 100029, China

Abstract Poly(vinylidene fluoride) (PVDF) and poly(butylene succinate-co-24 mol% hexamethylene succinate) (PBHS), both crystalline polymers, formed melt-miscible crystalline/crystalline polymer blends. Both the characteristic diffraction peaks and nonisothermal melt crystallization peak of each component were found in the blends, indicating that PVDF and PBHS crystallized separately. The crystalline morphology and crystallization kinetics of each component were studied under different crystallization conditions for the PVDF/PBHS blends. Both the spherulitic growth rates and overall isothermal melt crystallization rates of blended PVDF decreased with increasing the PBHS composition and were lower than those of neat PVDF, when the crystallization temperature was above the melting point of PBHS component. The crystallization mechanism of neat and blended PVDF remained unchanged, despite changes of blend composition and crystallization temperature. The crystallization kinetics and crystalline morphology of neat and blended PBHS were further studied, when the crystallization temperature was below the melting point of PBHS component. Relative to neat PBHS, the overall crystallization rates of the blended PBHS first increased and then decreased with increasing the PVDF content in the blends, indicating that the preexisting PVDF crystals may show different effects on the nucleation and crystal growth of PBHS component in the crystalline/crystalline polymer blends.

Keywords: Crystalline morphology; Crystallization kinetics; Polymer blends.

INTRODUCTION

Polymer blending is a useful and convenient way to produce materials with desired properties. The miscibility and crystallization behavior studies of amorphous/crystalline polymer blends have been reported extensively^[1–3]. However, crystalline/crystalline polymer blends have received much less attention. Till now, only a small number of works have been reported on the miscible polymer blends of two crystalline polymers with different chemical structures, which may provide various conditions to study the crystallization behavior and morphology of polymer blends^[4–23]. When the difference in melting point (T_m) is large, the two components cannot crystallize simultaneously but separately^[4–14]. However, the two components can crystallize simultaneously when the T_m difference is small^[15–20]. Much more attention has been paid to the crystallization and morphology of the high- T_m component in miscible crystalline/crystalline polymer blends; however, they actually become crystalline/amorphous polymer blends when the high- T_m component is crystallized at temperatures above T_m of the low- T_m component. Less attention has been directed to the crystallization and morphology of the low- T_m

^{*} This work was financially supported by the National Natural Science Foundation of China (No. 51221002).

^{**} Corresponding author: Zhao-bin Qiu (邱兆斌), E-mail: qiuzb@mail.buct.edu.cn

Invited paper for the special issue of “Polymer Crystallization”

Received March 6, 2014; Revised May 4, 2014; Accepted May 12, 2014

doi: 10.1007/s10118-014-1499-5

component, which are actually affected not only by blend composition and crystallization temperature but also by the preexisting crystals of high- T_m component in the blends.

In this work, we chose poly(vinylidene fluoride) (PVDF) and poly(butylene succinate-co-24mol% hexamethylene succinate) (PBHS) as the model system to study the crystalline morphology and crystallization kinetics of melt-miscible crystalline/crystalline polymer blends. The two components are both crystalline in their neat state and may undergo crystallization over a wide temperature range. We chose the PVDF/PBHS blend as a model system for the following two reasons. First, both poly(butylene succinate) (PBS) and its copolymer poly(butylene succinate-co-butylene adipate) (PBSA) have been reported to be miscible with PVDF^[8, 9, 12, 13]; therefore, it is expected that PBHS, a random copolyester of PBS and poly(hexamethylene succinate) (PHS), may also be miscible with PVDF. Second, the two components can only crystallize separately because of the large difference in the melting points between PVDF (~165 °C) and PBHS (~103 °C); therefore, the PVDF/PBHS blends may be an ideal system to study the crystalline morphology and crystallization kinetics of each component in their melt-miscible polymer blends.

EXPERIMENTAL SECTION

PVDF ($M_w = 1.8 \times 10^5$ g/mol) was purchased from Polysciences, Inc. PBHS ($M_w = 5.2 \times 10^4$ g/mol) was synthesized in our laboratory *via* a two-step melt polycondensation method^[24]. PVDF/PBHS blends were prepared through a solution and casting process using *N,N*-dimethylformamide (DMF) as the mutual solvent. The resulting films were dried in vacuum at 70 °C for 3 days to remove the solvent completely. PVDF/PBHS blends were prepared with various compositions ranging from 100/0, 85/15, 70/30, 50/50, 30/70, 15/85 to 0/100 in weight ratio, the first number referring to PVDF.

Wide-angle X-ray diffraction (WAXD) experiments were performed on a Rigaku D/Max 2500 VB2+/PC X-ray diffractometer at 40 kV and 200 mA from 5° to 45° at a scanning speed of 4 °/min. The samples for the WAXD experiments were crystallized at 70 °C for 24 h in an oven.

Thermal analysis was performed using a TA Instruments differential scanning calorimeter (DSC) Q100 with a Universal Analysis 2000 software. For both the nonisothermal and isothermal melt crystallization kinetics studies, the samples were first annealed at 190 °C for 3 min to reach the homogeneous melt state after erasing any previous thermal history. The detailed crystallization conditions were similar to those of PVDF/PBSA blends^[12, 13].

A polarizing microscope (POM) (Olympus BX51) equipped with a temperature controller (Linkam THMS 600) was used to investigate the crystalline morphology of PVDF/PBHS blends. Spherulitic growth rate (G) was studied by following the variation of radius (R) against crystallization time (t), *i.e.*, $G = dR/dt$.

RESULTS AND DISCUSSION

Miscibility and Crystal Structure Studies of PVDF/PBHS Blends

Both PVDF and PBHS are semicrystalline polymers. The basic thermal properties of them are as follows. PVDF has a glass transition temperature (T_g) of around -44.5 °C and a T_m of around 165 °C, while PBHS has a T_g of around -41.5 °C and a T_m of around 103 °C. The T_g values are so close to each other for the two components that the miscibility of PVDF/PBHS blends can not be confirmed by measuring a single composition dependent T_g as usual. In the present work, the miscibility of PVDF/PBHS blends was mainly evidenced by the homogeneous melt of the blend above T_m of PVDF. For brevity, the POM result is not shown here.

It is interesting to investigate the effect of blending with another crystalline component on the crystal structure of a component in crystalline/crystalline polymer blends. Figure 1 demonstrates the WAXD patterns of PVDF/PBHS blends. Both the neat components displayed characteristic diffraction peaks. Neat PVDF showed two strong diffraction peak at around 18.4° and 19.9°, corresponding to the α -form crystal of PVDF for (020) and (110) planes, respectively^[25], while neat PBHS also displayed two strong diffraction peaks at around 19.4° and 22.5°, corresponding to (020) and (110) planes, respectively^[24]. Figure 1 clearly shows that the WAXD

patterns involved all the main diffraction peaks, corresponding to each neat component in the blends. As a result, the co-crystallization did not occur in the PVDF/PBHS blends. PVDF and PBHS must crystallize separately in the blends; moreover, the intensity of the diffraction peaks of each component decreased with increasing the other component. In brief, blending with another crystalline polymer did not modify the crystal structure in the blends but only reduced the intensity of diffraction peaks.

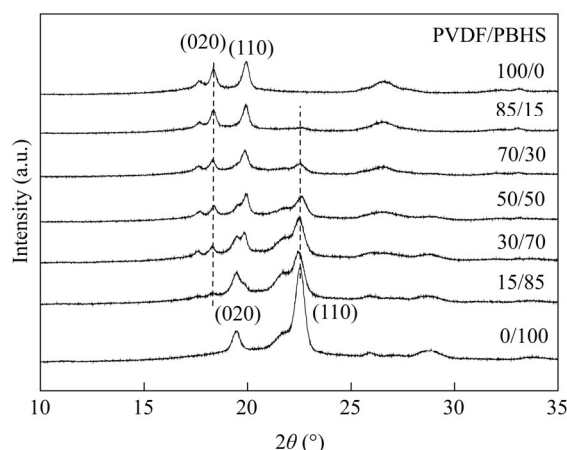


Fig. 1 WAXD patterns of PVDF/PBHS blends crystallized at 70 °C

Separate Crystallization of PVDF/PBHS Blends

In the above section, PVDF and PBHS were found to crystallize separately in the blends on the basis of the crystal structures study. In this section, DSC was further used to study the nonisothermal melt crystallization behavior of PVDF/PBHS blends. Figure 2 shows the DSC cooling traces of PVDF/PBHS blends at 10 K/min from the homogeneous melt. Neat PVDF showed a nonisothermal melt crystallization peak temperature (T_{cc}) at 137.5 °C, while neat PBHS had a T_{cc} of 63.4 °C. The difference between the T_{cc} values of the two neat components was more than 70 K. Figure 2 clearly illustrates that two crystallization exotherms were found at high and low temperature ranges for almost all the blends samples, corresponding to the crystallization processes of PVDF and PBHS, respectively. It should be noted that the crystallization exotherm of PBHS could not be found for the 85/15 blend, because of its small content and weak ability to crystallize. Therefore, it could be concluded that both the components crystallized separately in the PVDF/PBHS blends, which was consistent with the previous study. The crystallization exotherms of PVDF shifted gradually downward to low temperature ranges with increasing the PBHS component. As shown in Fig. 2, the T_{cc} value of PVDF was around 117.3 °C in the 15/85 blend, which was 20 K lower than that of neat PVDF. Such depression of T_{cc} should arise from the miscibility of PVDF/PBHS blends. While the T_{cc} values of PBHS in the blends shifted slightly downward to low temperature ranges with increasing the PVDF component. In addition to the variation of T_{cc} , the crystallization enthalpy (ΔH_{cc}) values were also obtained from Fig. 2. Neat PVDF had a ΔH_{cc} of 48.4 J/g, while in the blends the ΔH_{cc} values varied from 53.8 to 6.8 J/g with increasing the PBHS composition from 15 wt% to 85 wt%. On the basis of the heat of fusion of 100% crystalline PVDF (93.2 J/g)^[26], the degree of crystallinity value of neat PVDF was determined to be around 52%. The degree of crystallinity values of PVDF component were estimated to be around 63%~68% for the 85/15, 70/30, 50/50 and 30/70 blends and obviously decreased to be around 48% for the 15/85 sample, respectively, when they were normalized with respect to the PVDF composition in the blends. Neat PBHS had a ΔH_{cc} of 70 J/g. Because the heat of fusion of 100% crystalline PBHS has not been reported yet in the literature, the heat fusion of 100% crystalline PBS (140 J/g)^[27], was used to determine the degree of crystallinity values. For neat PBHS, the degree of crystallinity value was estimated to be around 50%. The degree of crystallinity values of PBHS component first increased to be around 56% for the 15/85 sample, decreased gradually with increasing the PVDF composition, and finally reached around 30% for the 70/30 sample, when they were normalized with respect to the PBHS composition in the blends.

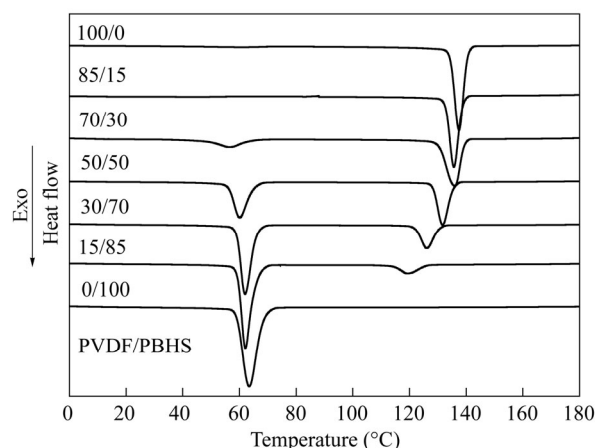


Fig. 2 DSC cooling traces of PVDF/PBHS blends at 10 K/min from the homogeneous melt

Spherulitic Morphology and Crystallization Kinetics of High- T_m Component PVDF in the Blends

Figure 3 illustrates a series of POM images for neat and blended PVDF, which were crystallized at 150 °C after erasing any previous thermal history. Regardless of blend composition, banded spherulites were found for all the samples; moreover, the band spacing was found to increase with increasing the PBHS composition. The band spacing was only about 3 μm for the PVDF spherulites of an 85/15 sample, while it was increased to be around 10 μm for those of a 50/50 sample. Similar results were also reported in the literatures^[12–14].

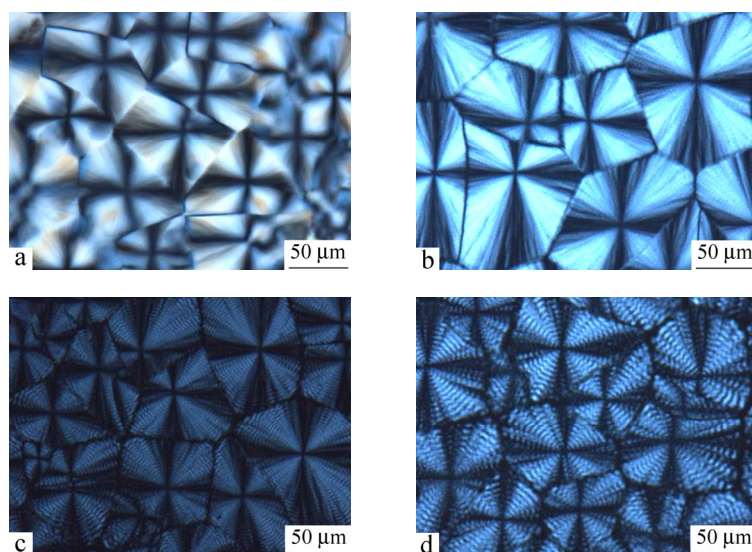


Fig. 3 Spherulitic morphology of PVDF component crystallized at 150 °C for (a) 100/0, (b) 85/15, (c) 70/30, and (d) 50/50 blends

Figure 4 summarizes the spherulitic growth rates of neat and blended PVDF crystallized at different crystallization temperature (T_c) values. As shown in Fig. 4, the G values decreased with increasing T_c for all the samples, regardless of blend composition; moreover, the G values were smaller in the blends than in neat PVDF at the same T_c . With increasing the PBHS composition, the G values decreased gradually at the same T_c . The reduction of the G values of PVDF spherulites were mainly attributed to the diluent effect of PBHS component in the blends, which is very common in miscible crystalline/amorphous polymer blends^[1–3].

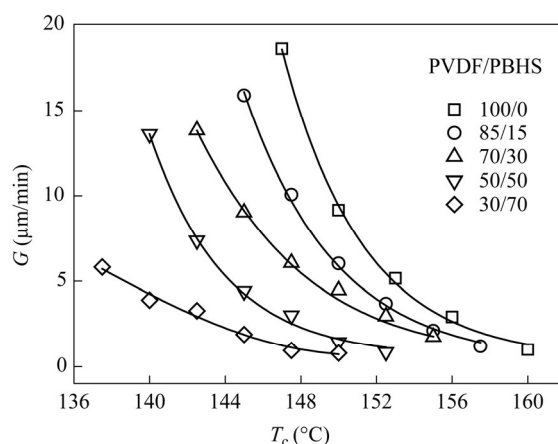


Fig. 4 Temperature dependence of spherulitic growth rates of neat and blended PVDF

The overall crystallization kinetics study was further performed at different T_c values after erasing any previous thermal history and analyzed by the well-known Avrami equation for neat and blended PVDF. According to the Avrami equation, relative degree of crystallinity (X_t) develops with crystallization time (t) as follows:

$$1 - X_t = \exp(-kt^n) \quad (1)$$

where n is the Avrami exponent depending on the nature of nucleation and growth geometry of the crystals, and k is the crystallization rate constant involving both nucleation and growth rate parameters^[28, 29]. Figures 5(a)–5(d) illustrate the Avrami plots for neat PVDF, 85/15, 70/30, and 50/50 blends crystallized at different T_c values, respectively. Figure 5 clearly shows that the isothermal melt crystallization processes of neat and blended PVDF may well be described by the Avrami method, because a series of almost parallel lines were obtained for each sample, regardless of blend composition and T_c ; therefore, the Avrami parameters n and k were calculated from the slopes and intercepts, respectively, and are summarized in Table 1 for comparison.

Within the investigated T_c range, the n values varied slightly between 2.1 and 2.8 for neat and blended PVDF. The slight variation of n values indicated that the crystallization mechanism of PVDF remained unchanged, regardless of blend composition and T_c . The average n value was around 2.5 for all the four samples, suggesting that neat and blended PVDF may all crystallize according to the three-dimensional truncated sphere growth with athermal nucleation mechanism^[30]. The k values are also listed in Table 1; however, they were not suitable to compare the overall crystallization rate directly, because the unit of them is min^{-n} and the n values were not the same for all the samples at different T_c values.

Therefore, the reciprocal of crystallization half-life time ($1/t_{0.5}$) was used in this work to compare the overall crystallization rate. The physical meaning of $t_{0.5}$ corresponded to the time required to achieve 50% of the final crystallinity of the samples, which could be calculated as follows on the basis of the Avrami equation:

$$t_{0.5} = \left(\frac{\ln 2}{k} \right)^{1/n} \quad (2)$$

For comparison, Table 1 also lists all the $t_{0.5}$ and $1/t_{0.5}$ values for neat and blended PVDF at different T_c values. Table 1 obviously shows that the $1/t_{0.5}$ values decreased with increasing T_c for each of the samples, indicating that the overall crystallization rate became slower at higher T_c because of smaller supercooling. At a given T_c of 142.5 or 145 °C, the $1/t_{0.5}$ values of the blends were smaller than that of neat PVDF and became smaller with increasing the PBHS content, indicating that the blending with PBHS suppressed the crystallization rate of PVDF. The T_c and blend composition dependences of overall crystallization rates of PVDF/PBHS blends were very common in miscible crystalline/amorphous polymer blends, because PBHS was actually in the melt and acted as a diluent during the crystallization of PVDF^[1–3].

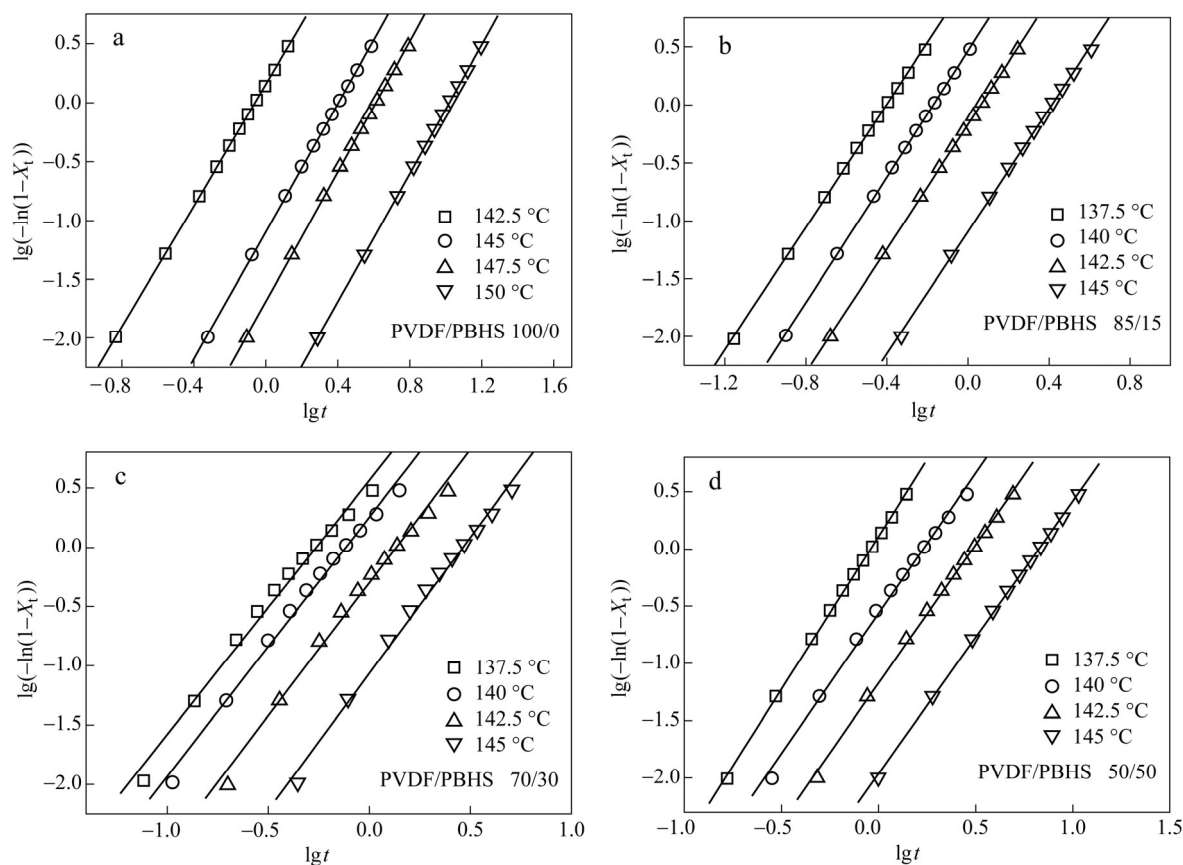


Fig. 5 Avrami plots of (a) 100/0, (b) 85/15, (c) 70/30 and (d) 50/50 PVDF/PBHS blends

Table 1. Avrami parameters for neat and blended PVDF at various T_c values

Samples	T_c (°C)	n	k (min ⁻ⁿ)	$t_{0.5}$ (min)	$1/t_{0.5}$ (min ⁻¹)
Neat PVDF	150	2.7	1.65×10^{-3}	9.15	0.11
	147.5	2.8	2.05×10^{-2}	3.58	0.28
	145	2.7	8.04×10^{-2}	2.21	0.45
	142.5	2.6	1.43	0.75	1.32
85/15	145	2.7	8.60×10^{-3}	2.26	0.44
	142.5	2.7	6.76×10^{-1}	1.01	1.00
	140	2.7	2.91	0.59	1.70
70/30	137.5	2.7	11.6	0.35	2.90
	145	2.3	8.52×10^{-2}	2.49	0.40
	142.5	2.2	4.98×10^{-1}	1.16	0.86
	140	2.2	1.79	0.65	1.54
50/50	137.5	2.1	3.64	0.46	2.17
	145	2.4	1.09×10^{-2}	5.73	0.17
	142.5	2.4	6.68×10^{-2}	2.62	0.38
	140	2.4	2.73×10^{-1}	1.46	0.68
	137.5	2.7	1.28	0.79	1.26

Crystallization Kinetics and Crystalline Morphology of Low- T_m Component PBHS in the Blends

In the above section, the effects of PBHS melt on the crystalline morphology and crystallization kinetics of PVDF were studied in detail for the PVDF/PBHS blends, which were actually melt-miscible crystalline/amorphous polymer blends. In this section, the effects of PVDF crystals on the crystallization kinetics and crystalline morphology of PBHS were further studied for the PVDF/PBHS blends, which were actually

melt-miscible crystalline/crystalline polymer blends. The overall isothermal melt crystallization kinetics of neat and blended PBHS was studied by DSC at different T_c values. Only two blend samples, *i.e.*, 30/70 and 15/85 were crystallized *via* a two-step crystallization process, which were crystallized during the second-step crystallization process after the crystallization of PVDF at 120 °C for 10 min during the first-step crystallization process from the homogeneous melt, whereas neat PBHS was directly crystallized *via* a one-step crystallization process from the homogeneous melt. Figure 6 shows the Avrami plots of neat and blended PBHS, from which the Avrami method was also found to be able to describe the isothermal melt crystallization process of PBHS, regardless of blend composition and T_c .

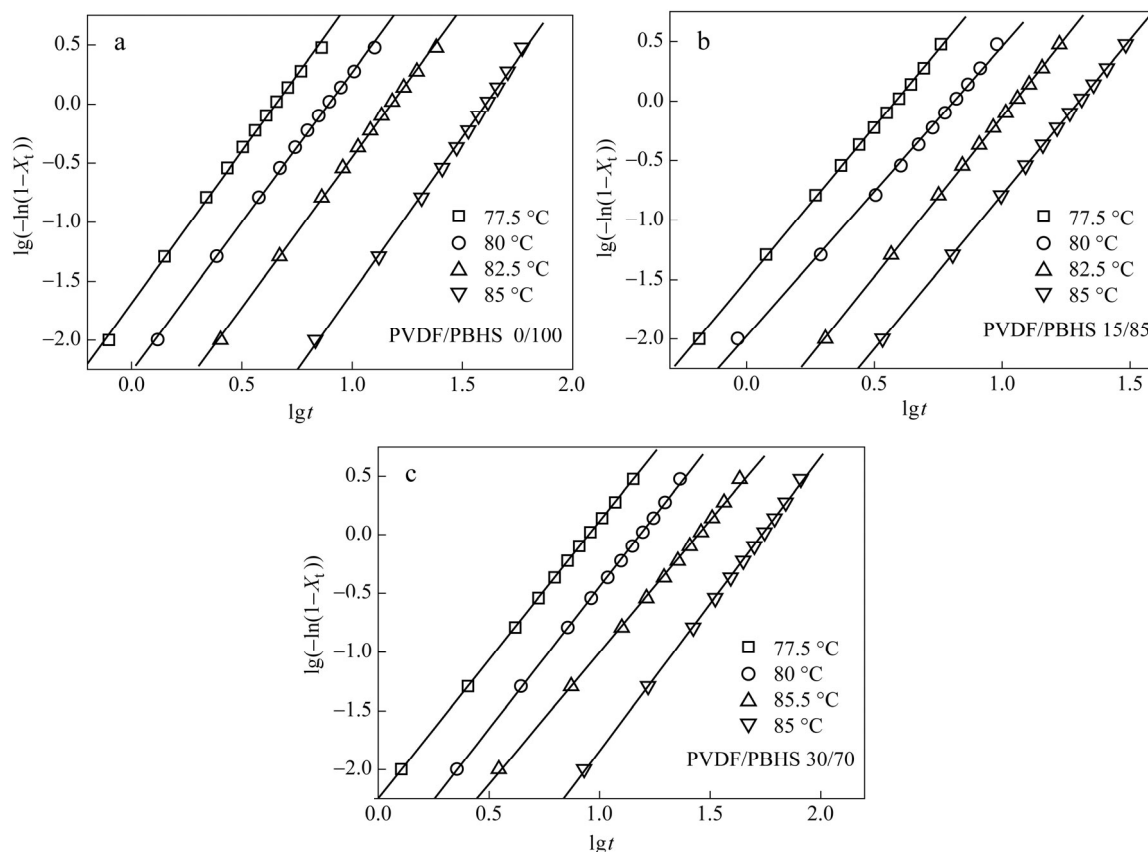


Fig. 6 Avrami plots of (a) 0/100, (b) 15/85, and (c) 30/70 PVDF/PBHS blends

For comparison, Table 2 lists all the n and k values of neat and blended PBHS at various T_c values. The n values varied slightly between 2.2 and 2.7 for neat and blended PBHS within the investigated T_c range, indicating that the crystallization mechanism of neat and blended PBHS may correspond to the spherulitic growth with three-dimensional truncated spheres and athermal nucleation^[30]. In brief, the almost unchanged n values indicated that the blending with PVDF did not affect the crystallization mechanism of PBHS, regardless of blend composition and T_c . Table 2 also lists the k values for neat and blended PBHS, which were also not suitable for the direct comparison of the overall crystallization rates for the same reason in the previous section. Therefore, the $1/t_{0.5}$ values were further used for the discussion of crystallization kinetics of neat and blended PBHS. Figure 7 illustrates the T_c dependence of $1/t_{0.5}$ for neat and blended PBHS, from which the following two trends were clearly obtained. On one hand, the $1/t_{0.5}$ values decreased with increasing T_c for all the samples, indicating a slower crystallization rate at higher T_c . On the other hand, at a given T_c , $1/t_{0.5}$ of neat PBHS was smaller than that of the 15/85 blend but greater than that of the 30/70 sample. With increasing the PVDF

composition from 15% to 30%, the overall crystallization rates of PBHS in the blends first increased and then decreased, relative to neat PBHS.

Table 2. Avrami parameters for neat and blended PBHS at various T_c values

Neat PBHS			15/85			30/70		
T_c (°C)	n	k (min ⁻ⁿ)	T_c (°C)	n	k (min ⁻ⁿ)	T_c (°C)	n	k (min ⁻ⁿ)
77.5	2.6	2.06×10^{-2}	77.5	2.6	3.13×10^{-2}	77.5	2.4	5.64×10^{-3}
80	2.5	5.42×10^{-3}	80	2.4	1.06×10^{-2}	80	2.4	1.36×10^{-3}
82.5	2.5	1.10×10^{-3}	82.5	2.7	1.54×10^{-3}	82.5	2.2	5.59×10^{-4}
85	2.6	5.87×10^{-5}	85	2.6	4.16×10^{-4}	85	2.5	4.45×10^{-5}

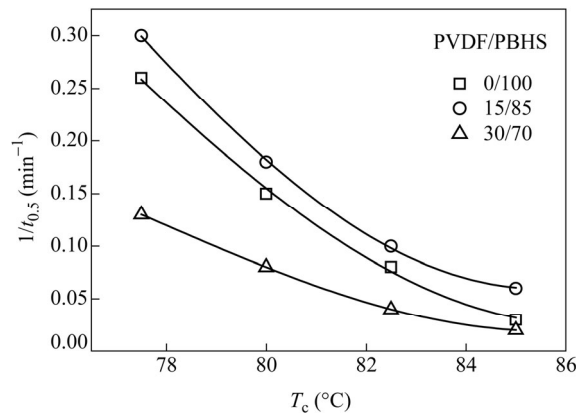


Fig. 7 T_c dependence of $1/t_{0.5}$ for neat and blended PBHS

In the above section, the overall crystallization rates of blended PBHS first increased and then decreased with increasing the PVDF composition. In this section, the crystalline morphology of blended PBHS was further studied with POM, which may provide some insights to the above variation of crystallization rates with blend composition. Figure 8 shows the crystalline morphology of neat and blended PBHS crystallized at 80 °C. All the samples exhibited spherulites morphology. Figure 8(a) clearly displays the typical negative spherulites of neat PBHS with clear boundaries. Figures 8(b) and 8(c) show that the blended PBHS spherulites were not as compact as those of neat PBHS ones, because they must crystallize in the presence of preexisting PVDF crystals, which may influence the regular spherulitic growth of PBHS in the blends. It is essential to compare the nucleation density and spherulitic growth rates of neat and blended PBHS. Figure 8 clearly shows that the nucleation density of PBHS spherulites first increased and then decreased with increasing the PVDF composition in the blends, relative to neat PBHS. The spherulitic growth rates of neat and blended PBHS were also measured. The spherulitic growth rate of the 15/85 blend was almost the same as that of neat PBHS, and their values were measured to be around 14.6 $\mu\text{m}/\text{min}$. However, the spherulitic growth rate of the 30/70 sample was only 9.9 $\mu\text{m}/\text{min}$, which was smaller than those of neat PBHS and the 15/85 blend. On the basis of the above nucleation and spherulitic growth rates information of neat and blended PBHS, the discussion of the overall crystallization rates of neat and blended PBHS should be more evident. Between neat PBHS and the 15/85 sample, the nucleation density of the latter was greater than that of the former; moreover, they had the similar spherulitic growth rates, thereby resulting in an enhanced overall crystallization rate of the 15/85 blend than that of neat PBHS. In the case of a 30/70 blend, its nucleation density and spherulitic growth rate values were both smaller than those of neat PBHS and the 15/85 blend, thereby resulting in the slowest overall crystallization rate among the three samples. In brief, the effects of preexisting PVDF crystals on the crystallization rates of PBHS of the blends may be summarized as follows. On one hand, depending on the blend composition, the preexisting PVDF crystals may enhance or decrease the nucleation density values of PBHS spherulites in the blends at low or high PVDF contents, respectively. On the other hand, the spherulitic growth rates of PBHS spherulites may

remain almost unchanged or decrease obviously at low or high PVDF contents in the blends. Thereby, the overall crystallization rates of PBHS in the blends first increased and then decreased with increasing the PVDF composition.

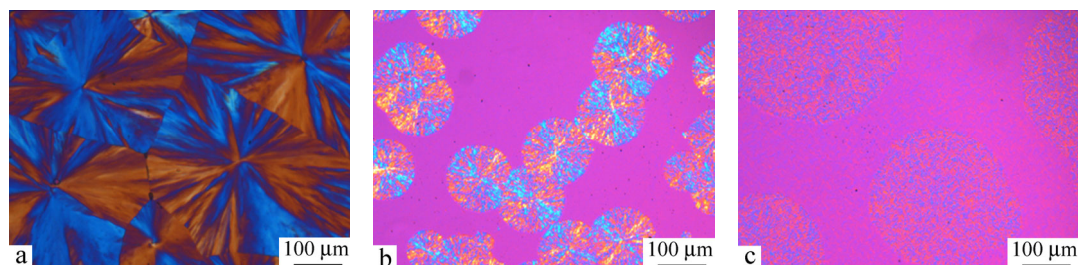


Fig. 8 Crystalline morphology of (a) neat PBHS, (b) 15/85, and (c) 30/70 PVDF/PBHS blends at 80 °C. The 15/85 and 30/70 samples were first crystallized at 120 °C for 10 min.

CONCLUSIONS

In the present work, the crystalline morphology and crystallization kinetics of each component were studied for the melt-miscible PVDF/PBHS blends. PVDF and PBHS were miscible because of the homogeneous melt above melting point of PVDF. Both the components crystallized separately, exhibiting their own crystal structures in the crystalline/crystalline polymer blends. When the samples were crystallized nonisothermally from the homogeneous melt, PVDF crystallized first at a high temperature range and PBHS then crystallized at a low temperature range in the blends; moreover, the depression of crystallization peak temperature of PVDF was obvious, while that of PBHS was slight, with increasing the blend composition of the other component in their blends. The spherulitic morphology and overall isothermal melt crystallization kinetics of neat and blended PVDF were first studied in a wide crystallization temperature range above melting point of PBHS. Under this condition, PVDF/PBHS blends were actually miscible crystalline/amorphous polymer blends, and PBHS actually acted as a diluent during the crystallization of PVDF in the blends. Both the spherulitic growth rates and overall isothermal melt crystallization rates of blended PVDF were smaller than those of neat PVDF and decreased with increasing the PBHS composition at the same crystallization temperature. Regardless of blend composition and crystallization temperature, the crystallization mechanism of neat and blended PVDF remained unchanged. The crystallization kinetics and crystalline morphology of neat and blended PBHS were further studied, when the blends were crystallized *via* a two-step crystallization process. Under this condition, PVDF/PBHS blends were actually melt-miscible crystalline/crystalline polymer blends. The effects of preexisting PVDF crystals on the crystallization kinetics and crystalline morphology of PBHS were investigated. Depending on the blend composition, the preexisting PVDF exhibited different influence on the nucleation density and growth rates of PBHS spherulites. At low PVDF composition, the overall crystallization rate of a 15/85 blend was faster than that of neat PBHS, whereas at high PVDF composition, the overall crystallization rate of a 30/70 was slower than that of neat PBHS.

REFERENCES

- 1 Cai, H., Yu, J. and Qiu, Z., *Polym. Eng. Sci.*, 2012, 52: 233
- 2 Yang, F., Li, Z. and Qiu, Z., *J. Appl. Polym. Sci.*, 2012, 123: 2781
- 3 Yang, F. and Qiu, Z., *Ind. Eng. Chem. Res.*, 2011, 50: 11970
- 4 Lee, J., Tazawa, H., Ikehara, T. and Nishi, T., *Polym. J.*, 1998, 30: 327
- 5 Qiu, Z., Ikehara, T. and Nishi, T., *Polymer*, 2003, 44: 2799
- 6 Qiu, Z., Fujinami, S., Komura, M., Nakajima, K., Ikehara, T. and Nishi, T., *Polymer*, 2004, 45: 4355

- 7 Ikehara, T., Kurihara, H., Qiu, Z. and Nishi, T., *Macromolecules*, 2007, 40: 8726
- 8 Wang, T., Li, H., Wang, F., Schultz, J. and Yan, S., *Polym. Chem.*, 2011, 2: 1688
- 9 Wang, T., Li, H., Wang, F., Yan, S. and Schultz, J., *J. Phys. Chem. B*, 2011, 115: 7814
- 10 Wang, H., Gan, Z., Schultz, J. and Yan, S., *Polymer*, 2008, 49: 2342
- 11 Wang, T., Wang, H., Li, H., Gan, Z. and Yan, S., *Phys. Chem. Chem. Phys.*, 2009, 11: 1619
- 12 Qiu, Z., Yan, C., Lu, J. and Yang, W., *Macromolecules*, 2007, 40: 5047
- 13 Qiu, Z., Yan, C., Lu, J., Yang, W., Ikehara, T. and Nishi, T., *J. Phys. Chem. B*, 2007, 111: 2783
- 14 Yang, J., Pan, P., Hua, L., Feng, X., Yue, J., Ge, Y. and Inoue, Y., *J. Phys. Chem. B*, 2012, 116: 1265
- 15 Qiu, Z., Ikehara, T. and Nishi, T., *Macromolecules*, 2002, 35: 8251
- 16 Lu, J., Qiu, Z. and Yang, W., *Macromolecules*, 2008, 41: 141
- 17 Ikehara, T., Kimura, H. and Qiu, Z., *Macromolecules*, 2005, 38: 5104
- 18 Yang, Y. and Qiu, Z., *Ind. Eng. Chem. Res.*, 2012, 51: 9191
- 19 Weng, M. and Qiu, Z., *Macromolecules*, 2013, 46: 8744
- 20 Wang, G. and Qiu, Z., *Ind. Eng. Chem. Res.*, 2014, 53: 1712
- 21 Schultz, J., *Front. Chem. China*, 2010, 5: 262
- 22 Lin, J. and Woo, E., *Polymer*, 2006, 47: 6826
- 23 Liu, J. and Jungnickel, B., *J. Polym. Sci. Part B: Polym. Phys.*, 2007, 45: 1917
- 24 Wang, G. and Qiu, Z., *Ind. Eng. Chem. Res.*, 2012, 51: 16369
- 25 Hasegawa, R., Takahashi, Y., Chatani, Y. and Tadokoro, H., *Polym. J.*, 1972, 3: 600
- 26 Welch, G. and Miller, R., *J. Polym. Sci., Polym. Phys. Ed.*, 1976, 14: 1683
- 27 Papageorgiou, G and Bikiaris, D., *Polymer*, 2005, 46: 12081
- 28 Avrami, M., *J. Chem. Phys.*, 1940, 8: 212
- 29 Avrami, M., *J. Chem. Phys.*, 1941, 9: 177
- 30 Wunderlich, B., "Macromolecular Physics" Academic Press, New York, 1976, Vol. 2